Manuscript refereed by Dr-Ing Núria Cinca (Hyperion Materials and Technologies, Spain)

Comparative Analysis of Methods for Determining the Critical Binder Volume Concentration in Hard Metal Pastes

Alexander Medina Peschiutta[1,2] alexander.medina@uni.lu; Marvin Just[1,2] marvin.just@ceratizit.com; Ralph Useldinger[2] ralph.useldinger@ceratizit.com; Jörg Baller[1] joerg.baller@uni.lu

[1]Department of Physics and Materials Science, University of Luxembourg, 162A Avenue de la Faiencerie, L-1511 Luxembourg, Grand Duchy of Luxembourg
[2]CERATIZIT Luxembourg S.à r.l., 101 Route de Holzem, L-8232, Grand Duchy of Luxembourg

Abstract

We present a comparative study on determining the critical binder volume concentration (CBVC) of a hard metal paste using the following techniques: theoretical calculation, density method, oil titration, binder titration, and Reddy's model. The theoretical calculations involve density measurements to discern the carbide powder-free volume. The titration methods consist of a stepwise increase of the organic content while the mixer torque is recorded. In contrast, Reddy's model requires the preparation of several feedstocks at varying solid loadings, which are tested in a capillary rheometer to obtain the CBVC. The paste consists mainly of nano-sized tungsten carbide-cobalt (powder phase) and a macromolecular multiphase system (organic phase). The accuracy and expenditure of experimental work of the different methods are discussed.

Introduction

Two main shaping routes are available in powder metallurgy: directly shaping the ready-to-press powder (RTP) or creating a paste that can be shaped. Each route presents its own advantages and disadvantages; the main advantage of pastes is the enabling of injection and extrusion techniques. Injection allows to manufacture parts with complex shapes, while extrusion is a cost-effective way to produce parts with constant cross-sections.

As shown in Figure 1, a paste is compounded by mixing powders with organic binders. To form a paste, the binder must replace the air between the powder particles. This process can take place in a high-shear mixer. It should be noted that the primary binder function is to keep the powder together after the shaping process, acting as a load carrier from the green until the brown stage, assisting in correctly shaping a defect-free part. In the next step, the binder is obliterated, and the composition of the final piece will consist purely of consolidated (by sintering) metallic or ceramic powder material.

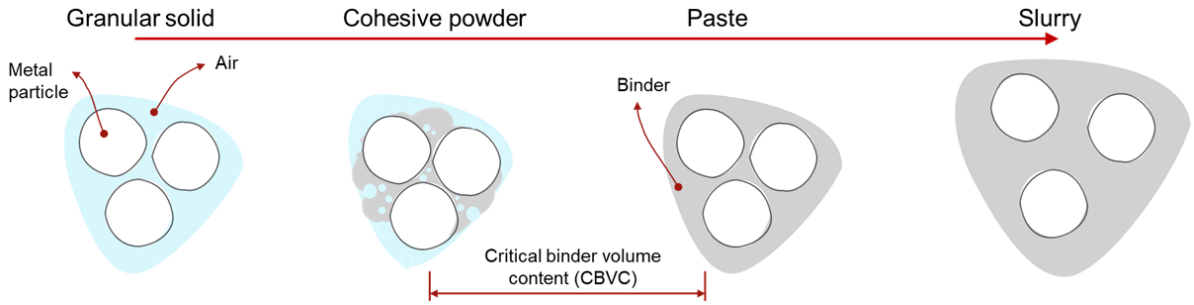

Figure 1. Schematic representation of the paste formation process as the organic binder content increases

The transient nature of the binder in the final part does not diminish its importance. Rather, its properties are crucial for achieving a defect-free product. Various shaping techniques such as extrusion, injection moulding, and extrusion-based additive manufacturing (EBAM) require specific binder properties for successful processing. In the following, some of the primary requirements for each technique are presented.

For extrusion, it is critical that the shape of the part remains stable after it exits the die. This means that the paste must not flow under the influence of gravitational forces. For injection, the paste needs a low

 https://doi.org/10.59499/EP235764669

viscosity presenting a shear thinning behaviour; this allows filling of the smallest corners of the mould cavities. In addition, the mould temperature can be reduced during the holding time to solidify one of the paste components and aid extraction by reducing the sticking forces with the mould. For EBAM, the extruder size is small and has a mechanical limit, meaning that the paste must have a low viscosity to enable the flow through nozzles of reduced diameters (0.3-0.8mm). Additionally, the paste must spread slightly after extrusion and hold its shape without creating surface defects. Finally, it must also stick to the subsequent layer using the thermal heat of the freshly extruded material.

The individual properties of the powder, the binder, and the interaction between them dominate the pastes' properties. While the powder composition is typically fixed according to final product requirements, the binder is the component that can be adjusted to allow for different production routes. When selecting a binder, it is important to consider several key criteria. Firstly, the binder should not alter the properties of the powder. Additionally, it should allow the powder to accurately replicate the geometry of the mould or die, maintain its shape during handling, and be easily removable during de-binding without introducing defects. In the paste processing industry, various binders are used. Some are water, cellulose, waxes, and polymers, often combined with surfactants, plasticisers, and emulsifiers.

Another crucial parameter is the quantity of binder in the paste. Using the minimum amount of binder that guarantees defect-free shaping and handling is beneficial because the part will experience less shrinkage during the sintering process. One way to optimise this parameter is by determining the critical binder volume concentration (CBVC), which is a widespread practice in ceramic and powder metallurgy. This quantity has been determined by a variety of methods for alumina [1]–[3], kaolin and alumina [4], zirconia [5], zirconium silicate [6], [7], stainless steel [5], [8]–[13], gas atomised Invar 36 alloy [14], [15], bonze and Inconel [16]–[18], carbonyl iron [19], titanium [20], [21], tungsten carbide [22]–[28] and other feedstocks. This paper focuses on the CBVC determination via various methods for a hard metal extrusion paste mainly comprised of nano-sized tungsten carbide, cobalt, and a proprietary organic binder.

Experimental

In most literature [1-28], the feedstocks are commonly prepared directly by mixing the metallic or ceramic powders with the binders in a kneader, extruder, or internal mixer. However, this study does not use pure powder as input for its feedstock, but uses ready-to-press (RTP) granules (see Figure 2). In short, the RTP granules are produced by means of attritor milling the metallic components (WC, Co and additives) with a milling agent (water, alcohol, or acetone) and a small quantity of organic binder (wax or polymers) to form a homogeneous slurry. Next, the slurry is spray-dried to evaporate the solvent, leading to the creation of the RTP granules.

RTP granules are beneficial because they guarantee a homogenous mixture of all constituents for the pressing process. Additionally, due to their spherical shape, they have better flow properties. The enhanced flow properties in the powder form are not relevant for extrusion or metal injection, but this is a crucial property for shaping techniques like isostatic die pressing, where RTP granules are directly shaped into a green part [33]. Figure 2 displays the difference between tungsten carbide powder and hard metal granules (RTP). For the system under study, an RTP granule can be seen as a homogeneous agglomerate of carbide particles, cobalt and a small quantity of organic binder. The nano size refers to the WC powder grain size, not the granule size.

 https://doi.org/10.59499/EP235764669

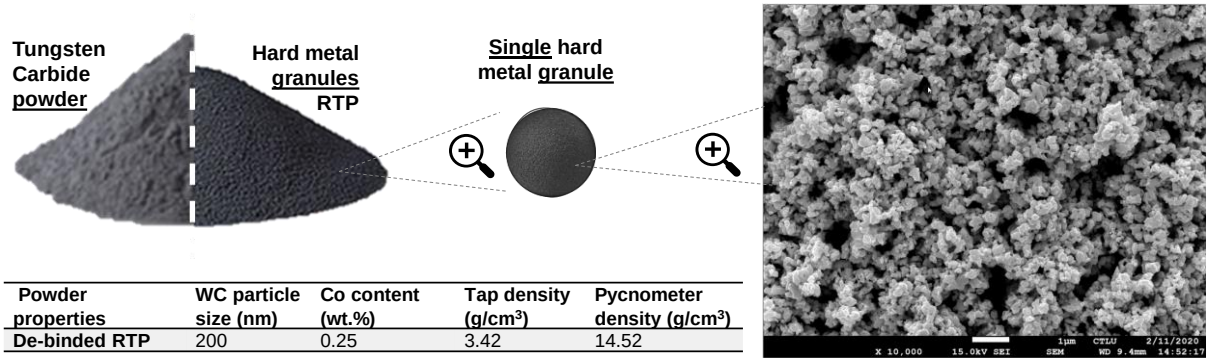

Powder properties	WC particle size (nm)	Co content (wt.%)	Tap density (g/cm³)	Pycnometer density (g/cm³)
De-binded RTP	200	0.25	3.42	14.52

Figure 2. Schematic representation of the physical characteristics of tungsten carbide powder and hard metal granules, along with an overview of the basic properties of the studied nano grain size hard metal powder system

Torque rheometry

The feedstocks were mixed using a BRABENDER PLASTICORDER kneader fitted with two sigma blades. The mixing chamber has a volume of ~1100 cm^3, enabling batches of ~2500 g of hard metal paste to be compounded (Figure 3). Two types of experiments were performed using the kneader, oil or binder titration and feedstock production for the capillary rheometer. For the later one, the mixing program had three stages: melting, kneading, and crushing. First, melting at 80 °C and 60 rpm until a paste is formed (~1 hour), followed by kneading at ~30 °C, 60 rpm for 5 hours and finally crushing or grinding the paste at 15 °C, 5 rpm for ~1 hour.

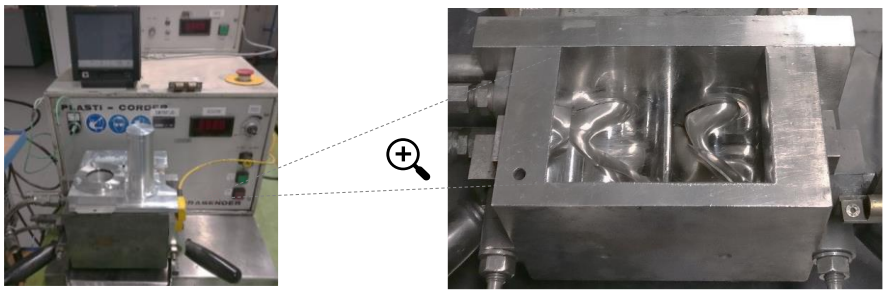

Figure 3. Kneader used for titration experiments and to create all the pastes analysed in this study

For most of the studies on hard metal pastes reported in literature [22], [23], [26]–[28], a mixing time under 1 hour suffices to spread the binder homogeneously throughout the powder surface. The mixing parameters used in this paper result from a series of experiments to optimize the mixing speed, time, and temperature (results not presented in this work). The longer mixing time of 7 hours for the powder used in this study is attributed to the nano-sized tungsten carbide particles, which require more time for proper dispersion within the mixture.

The following methods were used in the present paper to determine the CBVC:

Theoretical calculation

In Eq. 1, the critical particle volume concentration CPVC is the ratio between the tap density (ρ_{tap}) and the pycnometer density ($\rho_{pycnometer}$), of the powder without binder [34]. This ratio can be used as an indicator of the empty space between particles. The CBVC is obtained using Eq. 2. The tap density was measured with the device GRANUPACK from GRANUTOOLS (tap height 1mm, 500taps) and the pycnometer density with a helium pycnometer ACCUPYC II 1340 from MICROMERITICS.

$$CPVC = \frac{\rho_{tap}}{\rho_{pycnometer}} \quad \text{Eq. 1}$$

$$CBVC = 1 - CPVC \quad \text{Eq. 2}$$

 https://doi.org/10.59499/EP235764669

Density method

The density method is based on the concept that when the solid loading (powder) is increased, the binder may not fully embed the solid particles, leading to the presence of voids in the bulk material. Consequently, the measured density of the feedstock is smaller than the theoretical density [14], [29]. To determine the CBVC, this principle was applied by preparing several mixtures with increasing amounts of organic binder and measuring the density of the feedstock using a helium pycnometer. The CBVC is expected to occur at the point at which the density deviates from the mixing rule. For further details, please refer to [30].

Oil titration

The thermally de-bindered RTP powder is continuously mixed at 30 rpm and 30 °C in the mixer while small quantities of oil are added in 5 minutes intervals. The selected titration media was pure MAKANA Linseed oil for animals without additives. The resolution and length of the experiment depend on the titration step size. For this reason, the mixing started with 2060 g of powder and 100 ml of oil. Then, initial bigger oil aliquots of 5 ml were incorporated to the mix and when the powder started to appear wet (like in Figure 5, 51.2 vol.%) the step size was decreased to 2.5 ml to increase the resolution.

Proprietary binder titration

The CBVC may vary depending on factors such as the powder's surface chemistry, the viscosity of the titration media, and its wettability on the powder surface [30], [31]. Therefore, the CBVC was also determined using the proprietary binder mixture as titration media. Due to the multi-component nature of the binder system, a mother batch was prepared using a heat plate and a magnetic stirrer. First, all the organics were weighed and inserted into a beaker. Next, the components were mixed in a molten state for 5 minutes and cooled down until all the components solidified. Finally, the mother batch was used as a titration media adding it to the bulk (2060 g of powder) in steps of 1.5 g, starting from 4.00 to 6.10 wt.% (39.1 to 49.9 vol.%). For this, the mixing temperature was set above the melting points of all organic components (80 °C), a speed of 30 rpm and a time equilibrium between aliquots of approximately 5 minutes.

Reddy model

This method requires the preparation of at least three paste batches with varying binder content. All feedstocks should have a binder excess above the CBVC to be extrudable. For this study, five batches of 2000 g each were prepared and analyzed using the proprietary binder composition. The binder content of these batches ranged from 48.6 to 52.1 vol.%, with increments of 0.9 vol.%. Reddy et al. [31] propose to determine the critical binder volume content CBVC by measuring the viscosity (η) at a fixed shear rate and temperature for several binder volume contents BVC. The CBVC in Eq. 3 can be obtained from the slope. Additionally, since the critical powder volume content CPVC is equal to (1-CBVC), the binder viscosity without powder (η_b) can be derived from the intercept. The viscosity was measured using a capillary rheometer PORPOISE P9 fitted with a hard metal die with an orifice diameter of 1.5 mm and a length of 30mm.

$$\eta \cdot BVC = \eta \cdot CBVC + \eta_b \cdot CPVC \qquad \text{Eq. 3}$$

Results and discussion

Theoretical calculation

The current study uses carbide powder in the form of RTP granules, where the tap density measurement represents the void space between granules and not between individual nano-sized carbide particles. The obtained CBVC value is 76.5 vol.%, which was determined by measuring the tap and pycnometer density of the de-bindered RTP (Eq. 1 and Eq. 2). It is worth noting that the granules maintained their spherical shape after the thermal de-binding process. To refine the results, the tap density was re-measured using crushed (by mortar and pestle) de-bindered RTP, resulting in a slightly lower CBVC value of 73.3 vol.%. The astonishingly high CBVC values found by this method come from the fact that any modification of the powder during the mixing process is not considered. In fact, during mixing, the density of the mixture is greatly increased. The role of the binder at the first stages of mixing is mainly

 https://doi.org/10.59499/EP235764669

to transmit the shear forces which break the powder agglomerates, leading to a reduction of the voids and thus to an increase of density. In conclusion, this method is not suitable for the determination of the CBVC for this class of materials.

Density method

The density method was not effective for the system investigated in this study either. As shown in Figure 4 no discernible differences were observed between the theoretical and experimental density values. This can only be attributed to the fact that the measurement method used here (pycnometric measurement with helium as working gas) is able to consider any voids in the system. These findings are consistent with those reported by Abajo et al. [6], who attributed the imprecision of this method to the extremely irregular morphology (angular shape) of the powder particles and the presence of fine particles (1.94-5.49 µm) in a low viscosity binder system. On the contrary, Hidalgo et al. [14] investigated the critical loading using torque and density measurements on Invar 36 feedstock. They reported a difference of approximately 5 vol.% in the CPVC value depending on the technique used, with values of 67.5 and 62.5 vol.% obtained from torque and density measurements, respectively.

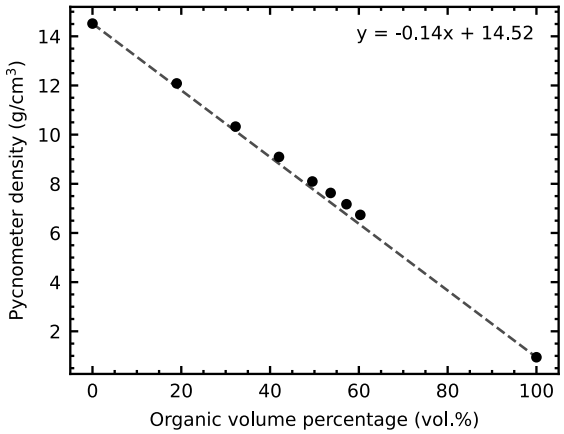

Figure 4. Feedstock density in function of the organic binder content. The dash line represents the theoretical densities according to a simple mixing rule.

Oil titration

Figure 5 showcases snapshots captured during the paste formation process in the kneader, providing visual insights into the effects of varying oil content on the behaviour of the bulk material. Notably, at 46.8 vol.% of linseed oil, the bulk material still behaves predominantly as a cohesive "dry" powder with visible lumps. However, with an increase in the ratio of organic binder (from 51.2 vol.% to 52.4 vol.%), the binder effectively binds more metal particles together, resulting in a visually wetter appearance of the bulk material and a rise in torque reading towards a maximum value (Figure 6). The maximum torque reading (53.8 vol.%) coincides with the formation of a coherent or continuous mass in the mixer, referred to as a paste, where the binder content is sufficient to keep most of the powder particles together. Nevertheless, the lack of binder for lubrication leads to increased particle-particle friction and, consequently, the highest torque readings. Subsequent incorporation of more binder reduces torque due to improved lubrication, which is advantageous for processing. Several researchers have reported that an optimal binder loading for the injection process lies within a binder excess of 2 to 5 vol% above the critical value [6], [16], [30], [32]. Beyond this optimal range, the paste properties tend towards the pure organic binder properties, and the paste transforms into a low-viscosity slurry-like material.

 https://doi.org/10.59499/EP235764669

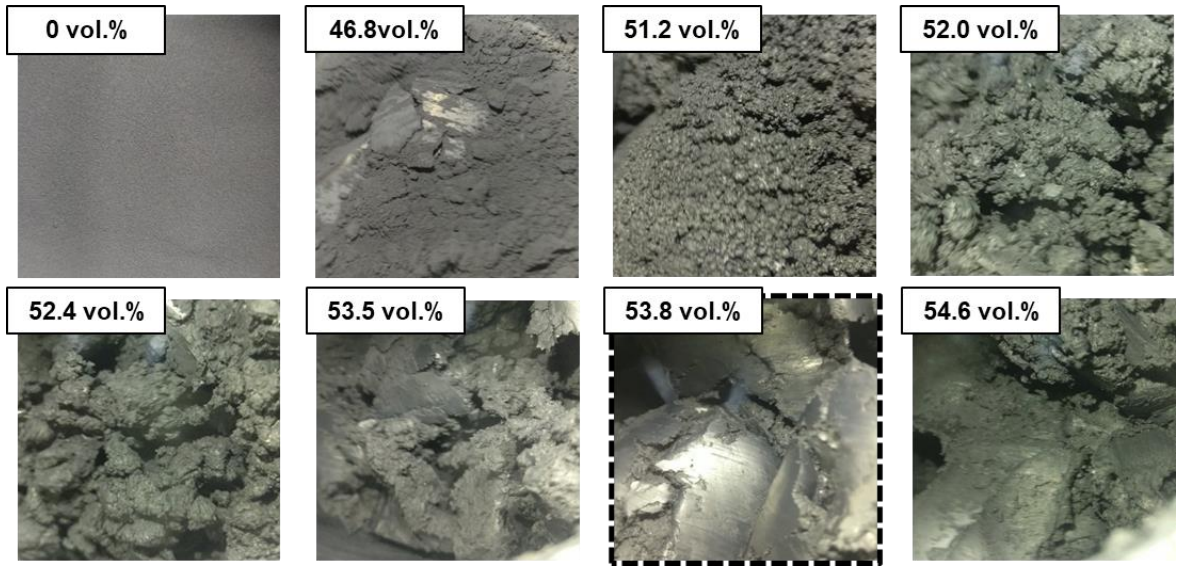

Figure 5. Linseed oil titration on dewaxed nano grain size hard metal powder. Images with increasing content of linseed oil from 0 to 54.6 vol.%. The CBVC correspond to the image with a black dashed frame (53.8 ± 0.4 vol.%).

Figure 6 presents the average torque obtained from 5 minutes of mixing with varying oil content, with error bars representing the deviation of torque values during a titration step. Three distinct regions are evident: (1) a stable region with minimal torque fluctuation up to 51.2 vol.% oil content, attributed to the system being predominantly in a powder-like form, (2) an intermediate region from 51.2 vol.% to 53.8 vol.% characterized by significant torque increase and higher variability, caused by the binder effect on powder particles agglomeration and paste formation, and (3) a region beyond the critical point where torque and variability decrease, indicative of reduced frictional forces due to excess binder. Finally, based on the oil titration method, the CBVC is estimated to fall within the 53.8 ± 0.4 vol.% range.

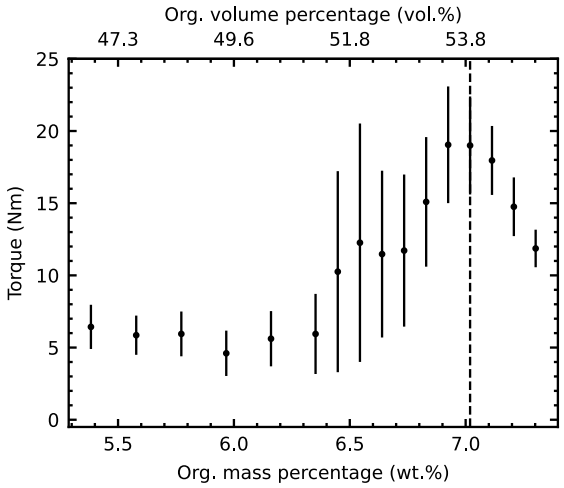

Figure 6. Titration of linseed oil on dewaxed nano grain size hard metal powder at 30 °C. Average torque readings (5 minutes) in the function of the organic content. The CBVC (53.8 ± 0.4 vol.%) is marked with a dashed vertical line.

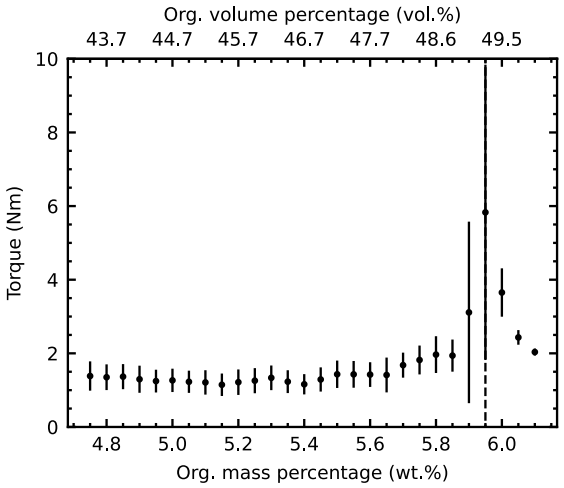

Figure 7. Titration of proprietary binder on nano grain size hard metal powder at 80 °C. Average torque readings (5 minutes) in the function of the organic content. The CBVC (49.3 ± 0.3 vol.%) is marked with a dashed vertical line.

Proprietary binder titration

The binder titration experiment was conducted using the proprietary organic binder mixture as titration media for the same hard metal system. Similar to the oil method, the CBVC was determined from the highest torque reading of Figure 7, corresponding to 49.3 ± 0.3 vol.% (5.95 ± 0.05 wt.%) of organic

 https://doi.org/10.59499/EP235764669

binder. The error corresponds to the binder addition step size. Furthermore, the transformation from powder to paste was observed to coincide with the highest torque reading, providing visual confirmation of the CBVC being within the postulated range.

Comparing the oil titration results with those obtained using the proprietary binder revealed a significant difference of 4.5 vol.% in the organic content at the CBVC. It is worth noting that the oil titration was performed at room temperature, while the binder titration was conducted at 80 °C. As higher temperatures promote wettability and lower viscosities, a fair comparison required repeating the oil titration at 80 °C, which reduced the difference to 3.0 vol.%. These findings emphasize the significant impact of binder properties on CBVC determination.

Reddy's model

The advantage of using Reddy's model over the titration method is that this technique delivers a CBVC value independent of the mixing parameters [31]. The five batches were analyzed in a capillary rheometer. For all compositions in Figure 8, shear thinning dominates the flow properties for the shear rate range studied (1 to 15 s^{-1}). A power law describes the data well; the fitting parameters are displayed in the legend.

The Reddy plot in Figure 9 is calculated from viscosity measurements at a single shear rate (11.5 s^{-1}) for all the concentrations. The CBVC is obtained from the slope of the linear fit using Eq. 3. Similarly, in Figure 10, the analysis is repeated for each shear rates present in Figure 8. If we look at the scale of Figure 10 and compare it to the previous methods, we could say that the CBVC determined via Reddy's model is shear rate independent. Therefore, the average CBVC is found to be 47.97 ±0.08 vol.%.

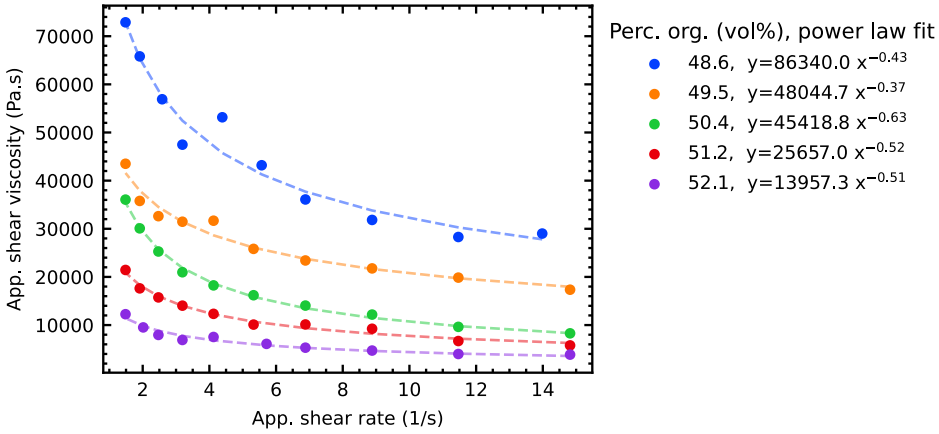

Figure 8. Flow curves from capillary rheometer at 32 °C with a die length of 30 mm and a diameter of 1.5 mm. Test performed from high to low shear rates with an initial pre-compaction step.

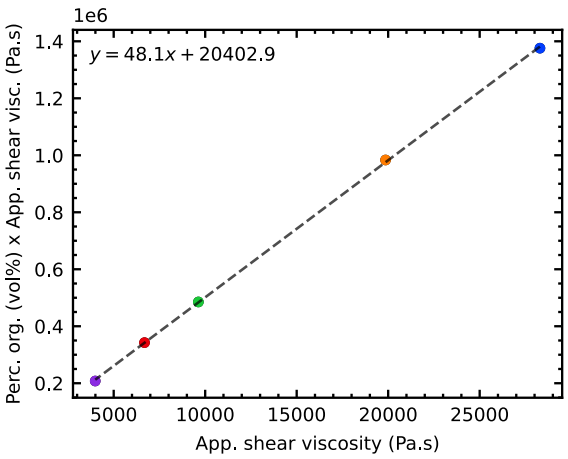

Figure 9. Reddy analysis at shear rate of 11.5 s^{-1}. Shared colour legend with Figure 8**.**

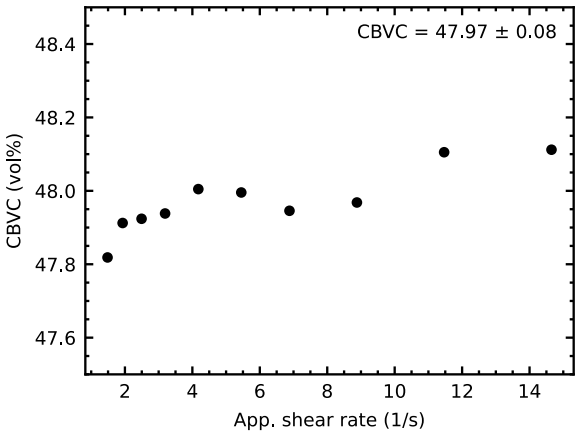

Figure 10. CBVC determined for each shear rate present in Figure 8

 https://doi.org/10.59499/EP235764669

Table 1: Summary of critical binder volume concentration (CBVC) determined via various methods for the nano-sized hard metal powder system

Method	Theoretical calculation	Oil titration (30 °C)	Oil titration (80 °C)	Binder titration (80 °C)	Reddy's model (32 °C)
CBVC (vol.%)	73	53.8 ± 0.4	52.3 ± 0.4	49.3 ± 0.3	47.97 ± 0.08

Conclusion

This study aims to investigate critical binder volume concentration (CBVC) using various methods, including theoretical calculation, oil titration, binder titration, and Reddy's model. The results reveal a consistent overestimation of CBVC by the theoretical and oil titration method compared to the binder titration and Reddy's model. For the oil titration, the discrepancies were attributed to differences in wettability and viscosity between oil and the proprietary binder. However, both binder titration and Reddy's model reveal similar results. It should be noted that the accuracy of the titration methods is dependent upon the size of the binder addition step, whereas Reddy's model is a more labour-intensive approach but is independent of this factor. These findings highlight the need for careful interpretation of CBVC results based on the employed method and emphasize the importance of utilizing the actual binder system in the paste under investigation for titration experiments.

Acknowledgements

This work was funded in whole, or in part, by the Luxembourg National Research Fund and by CERATIZIT Luxembourg S.à r.l. with two Industrial Fellowships grants. Grant acronyms and references are MEPFLOW [13320318] and RHAMEP [14187658].

References

[1] *J. Bricout, J. C. Gelin, C. Ablitzer, P. Matheron, and M. Brothier, "Influence of powder characteristics on the behaviour of PIM feedstock," Chem. Eng. Res. Des., vol. 91, no. 12, pp. 2484–2490, 2013, doi: 10.1016/j.cherd.2013.02.023.*

[2] *P. Thomas-Vielma, A. Cervera, B. Levenfeld, and A. Várez, "Production of alumina parts by powder injection molding with a binder system based on high density polyethylene," J. Eur. Ceram. Soc., vol. 28, no. 4, pp. 763–771, 2008, doi: 10.1016/j.jeurceramsoc.2007.08.004.*

[3] *E. Hnatkova, B. Hausnerova, and P. Filip, "Evaluation of powder loading and flow properties of Al2O3 ceramic injection molding feedstocks treated with stearic acid," Ceram. Int., vol. 45, no. 16, pp. 20084–20090, 2019, doi: 10.1016/j.ceramint.2019.06.273.*

[4] *F. Liu and K. Chou, "Determining critical ceramic powder volume concentration from viscosity measurements," Ceram. Int., vol. 26, pp. 159–164, 2000.*

[5] *Z. Chen, K. Ikeda, T. Murakami, and T. Takeda, "Effect of particle packing on extrusion behavior of pastes," J. Mater. Sci., vol. 35, no. 21, pp. 5301–5307, 2000, doi: 10.1023/A:1004834526344.*

[6] *C. Abajo, A. Jiménez-Morales, and J. M. Torralba, "Solid loading optimisation of extremely irregular particles," in Euro PM, 2014, [Online]. Available: https://www.epma.com/publications/euro-pm-proceedings/product/euro-pm2014-powder-injection-moudling-modelling-and-processing.*

[7] *J. Hidalgo, A. Jiménez-Morales, and J. M. Torralba, "Torque rheology of zircon feedstocks for powder injection moulding," J. Eur. Ceram. Soc., vol. 32, no. 16, pp. 4063–4072, 2012, doi: 10.1016/j.jeurceramsoc.2012.06.023.*

[8] *M. E. Sotomayor, B. Levenfeld, and A. Várez, "Powder injection moulding of premixed ferritic and austenitic stainless steel powders," Mater. Sci. Eng. A, vol. 528, no. 9, pp. 3480–3488, 2011, doi: 10.1016/j.msea.2011.01.038.*

[9] *J. M. Torralba, J. Hidalgo, and A. Jiménez-Morales, "Powder injection moulding: Processing of small parts of complex shape," Int. J. Microstruct. Mater. Prop., vol. 8, no. 1–2, pp. 87–96, 2013, doi: 10.1504/IJMMP.2013.052648.*

[10] *X. Kong, T. Barriere, and J. C. Gelin, "Determination of critical and optimal powder loadings for 316L fine stainless steel feedstocks for micro-powder injection molding," J. Mater. Process. Technol., vol. 212, no. 11, pp. 2173–2182, 2012, doi: 10.1016/j.jmatprotec.2012.05.023.*

[11] *M. E. Sotomayor, A. Varez, and B. Levenfeld, "Influence of powder particle size distribution on*

 https://doi.org/10.59499/EP235764669

rheological properties of 316L powder injection moulding feedstocks," Powder Technol., vol. 200, no. 1–2, pp. 30–36, 2010, doi: 10.1016/j.powtec.2010.02.003.

[12] M. H. I. Ibrahima, N. Muhamadband, and A. B. Sulongb, "Rheological Investigation of Water Atomised Stainless Steel Powder for Micro Metal Injection Molding," Int. J. Mech. Mater. Eng., vol. 4, no. 1, pp. 1–8, 2009, [Online]. Available: https://www.researchgate.net/publication/279580099_Rheological_investigation_of_water_atomised_stainless_steel_powder_for_micro_metal_injection_molding.

[13] B. Hausnerova, B. N. Mukund, and D. Sanetrnik, "Rheological properties of gas and water atomized 17-4PH stainless steel MIM feedstocks: Effect of powder shape and size," Powder Technol., vol. 312, pp. 152–158, 2017, doi: 10.1016/j.powtec.2017.02.023.

[14] J. Hidalgo, A. Jiménez-Morales, T. Barriere, J. C. Gelin, and J. M. Torralba, "Water soluble Invar 36 feedstock development for μPIM," J. Mater. Process. Technol., vol. 214, no. 2, pp. 436–444, 2014, doi: 10.1016/j.jmatprotec.2013.09.014.

[15] J. Hidalgo, A. Jiménez-Morales, T. Barriere, J. C. Gelin, and J. M. Torralba, "Capillary rheology studies of INVAR 36 feedstocks for powder injection moulding," Powder Technol., vol. 273, pp. 1–7, 2015, doi: 10.1016/j.powtec.2014.12.027.

[16] J. M. Contreras, A. Jiménez-Morales, and J. M. Torralba, "Experimental and theoretical methods for optimal solids loading calculation in MIM feedstocks fabricated from powders with different particle characteristics," Powder Metall., vol. 53, no. 1, pp. 34–40, 2010, doi: 10.1179/003258909X12450768327225.

[17] C. Dimitri, S. Mohamed, B. Thierry, and G. Jean-claude, "Influence of particle-size distribution and temperature on the rheological properties of highly concentrated Inconel feedstock alloy 718," Powder Technol., vol. 322, pp. 273–289, 2017, doi: 10.1016/j.powtec.2017.08.049.

[18] J. M. Contreras, A. Jiménez-Morales, and J. M. Torralba, "Fabrication of bronze components by metal injection moulding using powders with different particle characteristics," J. Mater. Process. Technol., vol. 209, no. 15–16, pp. 5618–5625, 2009, doi: 10.1016/j.jmatprotec.2009.05.021.

[19] S. M. Majdi, A. A. Tafti, V. Demers, G. Vachon, and V. Brailovski, "Effect of powder particle shape and size distributions on the properties of low-viscosity iron-based feedstocks used in low-pressure powder injection moulding," Powder Metall., vol. 0, no. 0, pp. 1–11, 2021, doi: 10.1080/00325899.2021.1959696.

[20] R. Côté, M. Azzouni, and V. Demers, "Impact of binder constituents on the moldability of titanium-based feedstocks used in low-pressure powder injection molding," Powder Technol., vol. 381, pp. 255–268, 2021, doi: 10.1016/j.powtec.2020.12.008.

[21] O. Ghanmi and V. Demers, "Molding properties of titanium-based feedstock used in low-pressure powder injection molding," Powder Technol., vol. 379, pp. 515–525, 2021, doi: 10.1016/j.powtec.2020.10.068.

[22] A. Fayyaz, N. Muhamad, A. B. Sulong, J. Rajabi, and Y. N. Wong, "Fabrication of cemented tungsten carbide components by micro-powder injection moulding," J. Mater. Process. Technol., vol. 214, no. 7, pp. 1436–1444, 2014, doi: 10.1016/j.jmatprotec.2014.02.006.

[23] B. Blackham, S. Blackburn, N. Rowson, and I. Al-Dawery, "The Effect Of Solids Loading On The Performance Of Extrusion Feedstock Of Cemented Carbide," in Euro PM, 2012, [Online]. Available: https://www.epma.com/publications/product/ep12326.

[24] S. N. A. Shahbudin, S. Y. M. Amin, M. H. Othman, and M. H. I. Ibrahim, "Critical powder loading and the rheology of Nanosized cemented carbide with titanium carbide as grain growth inhibitor for injection molding," Int. J. Integr. Eng., vol. 10, no. 4, pp. 114–118, 2018, doi: 10.30880/ijie.2018.10.04.019.

[25] S. Y. M. Amin, N. Muhamad, K. R. Jamaludin, A. Fayyaz, and H. S. Yunn, "Characterization of the Feedstock Properties of Metal Injection-molded WC-Co with Palm Stearin Binder System," Sains Malaysiana, vol. 43, no. 1, pp. 123–128, 2014, [Online]. Available: https://www.researchgate.net/publication/288221346_Characterization_of_the_Feedstock_Properties_of_Metal_Injection-molded_WC-Co_with_Palm_Stearin_Binder_System.

[26] B. Hausnerová, P. Sáha, and J. Kubát, "Capillary Flow of Hard-Metal Carbide Powder Compounds," Int. Polym. Process., vol. 14, no. 3, pp. 254–260, 1999, doi: 10.3139/217.1556.

[27] B. Hausnerova, P. Sáha, J. Kubát, T. Kitano, and J. Becker, "Rheological behaviour of hard-metal carbide powder suspensions at high shear rates," J. Polym. Eng., vol. 20, no. 4, pp. 237–266, 2000, doi: 10.1515/POLYENG.2000.20.4.237.

[28] A. Fayyaz, N. Muhamad, A. B. Sulong, H. S. Yunn, S. Y. M. Amin, and J. Rajabi, "Micro-powder injection molding of cemented tungsten carbide: Feedstock preparation and properties," Ceram. Int., vol. 41, no. 3, pp. 3605–3612, 2015, doi: 10.1016/j.ceramint.2014.11.022.

[29] J. J. Reddy, M. Vijayakumar, T. R. R. Mohan, and P. Ramakrishnan, "Loading of Solids in a

Liquid Medium: Determination of CBVC by Torque Rheometry," J. Eur. Ceram. Soc., vol. 16, no. 5, pp. 567–574, 1996, doi: 10.1016/0955-2219(95)00165-4.

[30] R. M. German and A. Bose, Injection Molding of Metals and Ceramics. New Jersey: Metal Powder Industries Federation, 1997.

[31] J. J. Reddy, N. Ravi, and M. Vijayakumar, "A simple model for viscosity of powder injection moulding mixes with binder content above powder critical binder volume concentration," J. Eur. Ceram. Soc., vol. 20, no. 12, pp. 2183–2190, 2000, doi: 10.1016/S0955-2219(00)00096-0.

[32] J. W. Oh, R. Bollina, W. S. Lee, and S. J. Park, "Effect of nanopowder ratio in bimodal powder mixture on powder injection molding," Powder Technol., vol. 302, pp. 168–176, 2016, doi: 10.1016/j.powtec.2016.08.051.

 https://doi.org/10.59499/EP235764669